

Film Formation of Two-Stage Acrylic Latexes: Toward Soft-Core/Hard-Shell Systems

Elvis Lopes Brito and Nicholas Ballard*

Controlling the colloidal structure of multiphase latex particles offers a route to significant improvements in the mechanical properties of dried films for use in coatings. However, there is often conflict between the morphology that leads to optimum mechanical properties and the morphology that ensures good film formation at reduced temperatures. In this work, the case of two-stage latex particles in which the second-stage polymer has a high glass transition temperature (T_g) is considered. First, a number of different core/shell-like particles with different polymer compositions and particle structures are synthesized by seeded semi-batch emulsion polymerization. Using these latexes, the importance of phase mixing, particle morphology, and polymer composition with respect to film formation behavior and mechanical performance is discussed. The results highlight that in multiphase latex systems, the film formation behavior is dictated by the interplay between various colloidal and polymeric features of the samples. It is shown that understanding these features offers a route to systems that can match the film formation properties of a low T_g latex, whilst also approaching the mechanical properties of a high T_g polymer.

systems, only polymers with a glass transition temperature (T_g) close to or below that of the casting temperature can readily form a film.^[4,5] This puts significant restrictions on the final mechanical properties of the film and in particular on the modulus, which plays a major role in blocking resistance,^[6] thereby limiting the use of waterborne systems in many high-performance protective coatings. The reduced mechanical performance of waterborne systems is therefore a challenge that must be overcome if solvent-based coatings are to be further phased out of use.

To overcome the issue of limited mechanical performance, a number of alternatives have been proposed including the use of inorganic/polymer hybrids,^[7–10] chemical^[11–14] and physical^[15–19] crosslinking of the polymer after film formation, and the use of multiphase latexes.^[20–24] Multiphase systems contain a high T_g polymer to improve mechanical performance and a low T_g polymer to aid in film formation.


These multiphase latexes are generally synthesized by a two-stage emulsion polymerization process using two different monomer compositions and can lead to particles of various equilibrium and non-equilibrium morphologies. When using multiphase latexes, the composition of each phase is important but the morphology plays an arguably more important role. For example, when the low T_g component is in the shell, the minimum film formation temperature (MFFT) is relatively unaffected up to high hard phase content, but the improvement in mechanical performance is limited.^[22,25] By promoting the enrichment of the hard phase at the particle surface, significant increases in mechanical performance can be obtained at the expense of an increase in the MFFT.^[26–28] Thus even for identical polymer phases, the initial particle morphology can massively influence both film formation and mechanical properties of the films.

In this work, we look at the use of two-stage latex systems in which the second-stage polymer has a high T_g . Previous work using similar latexes has led to conflicting results, even for relatively similar formulations. For example, Leibler and co-workers reported the synthesis of a poly(butyl acrylate)-core/poly(methyl methacrylate) shell system.^[28,29] In their work, it was supposed that the morphology was a true core-shell system and the final film morphology, analyzed by TEM, indicated a percolating network of the high T_g poly(methyl methacrylate) phase. This percolating structure led to films with an exceptionally high

1. Introduction

Waterborne polymer dispersions have been widely used in the coatings industry since the 1950s.^[1] Unlike the solvent-based polymers that have traditionally dominated the coatings market, waterborne systems contain limited volatile organic content and therefore offer significant environmental advantages.^[2,3] However, due to the mechanism of film formation of waterborne

E. Lopes Brito, N. Ballard
 POLYMAT – University of the Basque Country UPV/EHU
 Joxe Mari Korta zentroa, Tolosa Hiribidea 72, Donostia-San Sebastián
 20018, Spain
 E-mail: nicholas.ballard@polymat.eu
 N. Ballard
 Ikerbasque
 Basque Foundation for Science
 Bilbao 48013, Spain

 The ORCID identification number(s) for the author(s) of this article can be found under <https://doi.org/10.1002/mame.202300287>

© 2023 The Authors. Macromolecular Materials and Engineering published by Wiley-VCH GmbH. This is an open access article under the terms of the Creative Commons Attribution License, which permits use, distribution and reproduction in any medium, provided the original work is properly cited.

DOI: 10.1002/mame.202300287

Table 1. Composition of the core latexes.

Codes	Small-seed latexes					Large-seed latexes			
	S_a	S_b	S_c	S_d	S_e	L_a	L_b	L_c	
Initial Charge	Reagent	Amount [g]					Amount [g]		
	Seed			0			7 (S_a)	7 (S_b)	7 (S_c)
	Water			220				120	
Initiator solution	SDS			1.5				–	
	Water			20				–	
	KPS			0.95				–	
Monomer feed	Reagent	Amount [g]					Amount [g]		
	Water	420	420	420	420	420	575	575	575
	SDS	4	4	4	4	4	4.38	4.38	4.38
	MMA	–	–	–	142	237	–	–	–
	BA	475	475	475	333	237	487	487	487
	BDA	0	0	2.9	0	0	–	2.97	–
	TDM	0	0.475	0	0	0	–	–	0.535
KPS	0	0	0	0	0	0.97	0.97	0.97	

modulus, even when the poly(methyl methacrylate) fraction was low (20 wt%). Using an almost identical synthetic procedure but with significantly larger initial seed particles, Sommer et al. demonstrated that the latex did not form a true core/shell type structure but rather resulted in a raspberry-like morphology with clusters of poly(methyl methacrylate) at the surface.^[30] In agreement with this latter study, Asua and co-workers have shown that across a wide range of core and shell compositions, the morphology was a patchy structure with the high T_g second-stage polymer present at the particle surface.^[27,31,32] As a result of the non-continuous shell layer, the MFFT remained low but the dried film still exhibited a significant increase in the modulus.

Here, we explore how subtle changes to the particle structure of two-stage emulsion polymers can influence both the mechanical properties of the final film as well as the film formation behavior. To do so, a series of latexes have been synthesized in which the core is composed of a butyl acrylate (BA)-rich copolymer of varying T_g and particle size, and the second stage polymer is made up of a methyl methacrylate (MMA)-rich copolymer of varying T_g with varying volume fractions relative to the core. First, the synthesis of these systems by two-stage semi-batch emulsion polymerization is reported. Subsequently, the film formation behavior and the mechanical properties of the dried films are compared.

2. Experimental Section

2.1. Materials

The monomers used in this work, MMA (technical grade, Quimidroga), styrene (S, technical grade, Quimidroga), and BA (technical grade, Quimidroga) were used without any further purification. Potassium persulfate (KPS, >98%, Sigma Aldrich), sodium dodecyl sulfate (SDS, >98%, Sigma Aldrich), 1,4-butanediol diacrylate (BDA, >98%, Sigma Aldrich), and tert-

dodecylmercaptan (TDM, >98%, Sigma Aldrich) were used as supplied. Deionized water was used throughout the work.

2.2. Synthesis of Seed Latexes

Semi-batch emulsion polymerization was used to synthesize the BA, MMA/BA 30/70 wt/wt, and MMA/BA 50/50 wt/wt latexes in a 1 L jacketed glass reactor equipped with a nitrogen inlet, a thermocouple, a condenser, and a stainless steel anchor-type stirrer. The composition of the latex can be found in **Table 1**. For the synthesis of the small-seed latexes, the reactor was loaded with the initial charge, and the temperature was raised to 80 °C under nitrogen flux and continuous stirring (250 rpm). After the temperature was equilibrated, the initiator solution was added as a shot. The resultant solution was stirred for 5 min, and then the feeding of the pre-emulsion was started and completed in 180 min. The system was held at the reaction temperature for an additional 60 min. The large-seed latexes were prepared by seeded semi-batch emulsion polymerization, using the previously synthesized small-seed latex particles as a seed. As shown in **Table 1**, the latexes were coded based on the particle size (small, S, or large, L) and the monomer feed composition (a–e). Composition a was exclusively butyl acrylate. Composition b contained 0.1 wt% of TDM as a chain transfer agent. Composition c contained 0.6 wt% of BDA as a crosslinker. Compositions d and e were copolymers of MMA and BA with composition MMA/BA 30/70 and 50/50 wt/wt, respectively.

2.3. Synthesis of Two-Stage Latex Particles

A series of two-stage latex particles composed of a low T_g seed and a high T_g second-stage polymer was synthesized via seeded semi-batch emulsion polymerization (**Table 2**). The small and large latexes reported in **Table 1** were used as seeds. Parameters, such as the composition of the hard phase and the ratio of soft/hard

Table 2. Composition of two-stage latex particles.

	Samples Code	Ratio Core/shell	Seed		Initiator solution		Monomer feed		
			Type	Amount [g]	KPS [g]	Water [g]	MMA [g]	S [g]	EA [g]
Small particles	S _a 1-20	80/20	S _a	100	0.05	15	8.7	1.6	–
	S _a 1-30	70/30	S _a		0.08	20	14.5	2.5	–
	S _a 1-35	65/35	S _a		0.10	25	18.3	3.2	–
	S _a 2-30	70/30	S _a		0.08	20	12	2.5	2.5
	S _a 3-30	70/30	S _a		0.08	20	9.4	2.5	5.1
	S _a 4-30	70/30	S _a		0.08	20	7.25	2.5	7.25
	S _b 1-20	80/20	S _b		0.05	15	8.7	1.6	–
	S _b 1-30	70/30	S _b		0.08	20	14.5	2.5	–
	S _c 1-20	80/20	S _c		0.05	15	8.7	1.6	–
	S _d 1-20	80/20	S _d		0.05	15	8.7	1.6	–
Large particles	S _e 1-20	80/20	S _e		0.05	15	8.7	1.6	–
	L _a 1-20	80/20	L _a		0.05	15	8.7	1.6	–
	L _a 1-30	70/30	L _a		0.08	20	14.5	2.5	–
	L _a 1-35	65/35	L _a		0.10	25	18.3	3.2	–
	L _a 4-30	70/30	L _a		0.08	20	7.25	2.5	7.25
	L _b 1-20	80/20	L _b		0.05	15	8.7	1.6	–
	L _b 1-30	70/30	L _b		0.08	20	14.5	2.5	–
	L _c 1-20	80/20	L _c		0.05	15	8.7	1.6	–

polymer, were explored. The composition of the hard phase polymer was varied by changing the MMA/EA content with a constant fraction of 15% (w/w) of styrene in all the samples. The synthesis was carried out by adding the required amount of seed to the reactor and heating it to 80 °C under nitrogen flux with stirring at 250 rpm. After the temperature stabilized, the initiator solution was added as a shot. The amount of water in the initiator solution was adjusted to give final latexes with comparable solid contents. The monomer solution was fed for 30 min. Following monomer addition, the reaction temperature was held for an additional hour in order to ensure complete polymerization. The reaction codes in Table 2 correspond to the type of seed used (small, S, or large, L with composition a–e) and composition (1–4) and weight percentage of second-stage polymer (20–40). For example, sample S_a 4-30 corresponded to a latex that was synthesized using seed S_a (small seed with composition “a” (100% butyl acrylate)) with 30 wt% of a second stage polymer with composition 4 (MMA/EA/S 42.5/42.5/15 wt/wt/wt).

2.4. Latex Characterization

The solids content and monomer conversion were determined by gravimetry. Particle sizes were measured by dynamic light scattering (DLS) in a Zetasizer Nano Z (Malvern instruments). Samples were prepared by diluting a fraction of latex with deionized water. The equipment was operated at 25 °C and the reported values were the size distribution as a function of intensity for three repeated measurements.

The gel content of the polymer was measured using Soxhlet extraction for 24 h with tetrahydrofuran (THF) as solvent. The

gel content was defined as the insoluble fraction of the polymer in THF. The molecular weights of the soluble fraction of the polymers were determined by gel permeation chromatography (GPC). The soluble part of the polymers from the Soxhlet extraction was dried and redissolved in GPC grade THF at a concentration of roughly 2 mg mL⁻¹. The solution was filtered (polyamide Φ = 45 μm) before being injected into the GPC via an autosampler (Water 717). A pump (LC-20A, Shimadzu) controlled a THF flow of 1 mL min⁻¹. The GPC was composed of a differential refractometer (Waters 2410) and three columns in series (Styragel HR2, HR4, and HR6, with pore sizes ranging from 10² to 10⁶ Å). Measurements were performed at 35 °C. Molecular weights were determined using a calibration curve based on polystyrene standards.

The glass transition temperature was determined by differential scanning calorimetry (DSC) Q2000 modulated DSC (TA instruments). The samples were dried at 22 °C (55% of relative humidity) and about 8 mg of the polymer was added to the respective pan. The pans were then sealed and the analysis was carried out with two heating/cooling cycles from –80 to 150 °C with a heating rate of 10 °C min⁻¹.

Particle morphologies were determined by transmission electron microscopy (TEM) using a Jeol TM-1400 Plus series 120 kV electron microscope. The latexes were diluted with deionized water (0.05 wt%) placed on copper grids covered with Formvar R and dried at low temperatures. Thereafter, the samples were stained with vapor of RuO₄ for 20 min. In the case of the film, slices of the film were prepared in a microtome equipped with a diamond knife at –25 °C and then deposited on the copper grids. Similar to the dispersions, the film was stained with vapor of RuO₄ for 10 min.

Table 3. Characteristics of seeds and two-stage latexes.

Sample	Particle size [nm]	PDI	Sol M_w [g mol ⁻¹]	\bar{D}	Gel content [%]	Seed polymer T_g [°C]	Second stage polymer T_g [°C]
S _a	68	0.041	5.6×10^4	2	72	-42	-
S _b	67	0.061	7.5×10^4	2.1	<5	-42	-
S _c	69	0.035	5.6×10^4	1.9	78	-42	-
S _d	79	0.038	6.6×10^5	7.4	8	-13	-
S _e	78	0.067	1.1×10^5	9.5	9	20	-
L _a	363	0.005	2.5×10^5	3.7	66	-47	-
L _b	366	0.020	4.7×10^5	6.3	<5	-47	-
L _c	369	0.035	4.8×10^5	6.4	88	-47	-
S _a 1-20	73	0.064	7.4×10^4	2.1	60	-42	115
S _a 1-30	75	0.042	2.2×10^5	4.1	54	-42	117
S _a 1-35	86	0.078	2.3×10^5	3	58	-42	116
S _a 2-30	76	0.039	2.2×10^5	4.6	65	-42	93
S _a 3-30	76	0.067	2.2×10^5	4.9	63	-42	72
S _a 4-30	75	0.080	1.7×10^5	3.4	57	-42	55
S _b 1-20	73	0.064	1.4×10^5	3	<5	-42	113
S _b 1-30	75	0.042	2.5×10^5	4	<5	-42	115
S _c 1-20	72	0.062	1×10^5	2.8	72	-42	109
S _d 1-20	84	0.046	5.9×10^5	7	<5	-13	108
S _e 1-20	83	0.081	2.3×10^5	8.6	<5	20	112
L _a 1-20	375	0.039	2×10^5	3.8	55	-47	109
L _a 1-30	393	0.032	2.4×10^5	3.1	60	-47	110
L _a 1-35	401	0.022	3.5×10^5	3.9	58	-47	112
L _a 4-30	396	0.032	2×10^5	4.2	61	-47	52
L _b 1-20	376	0.030	3.6×10^5	5.7	<5	-47	112
L _b 1-30	390	0.041	4.7×10^5	6.1	<5	-47	113
L _c 1-20	375	0.039	1.5×10^5	3.5	74	-47	112

2.5. Film Characterization

Latex films were prepared by casting 3 g of latex (solids contents 40%) in rectangular silicone molds (26 mm × 56 mm) and letting them dry at 23 °C and 55% relative humidity for 5 days. The final film thickness was around 0.9 mm.

The MFFT measurements were performed using an MFFT-Bar (model 90 from Rhopoint) with a range of temperatures from 0 to 90 °C based on the MFFT measurement described in ISO 2115. All the films were cast using a film applicator with 200 μm wet thickness. The MFFT was measured after 2 h and was defined as the point at which continuous homogeneous films without any cracks were observed.

Tensile stress–strain measurements were carried out for the latex films with a tensile testing machine (Stable Micro Systems Ltd., Godalming, UK) with a constant velocity of 0.42 mm s⁻¹. The results reported were the average of 2–3 repeated measurements.

The thermomechanical behavior of the latex films was investigated by a dynamic mechanical analyzer (DMA), using a Triton 2000 DMA from Triton technology. The tension mode was selected and constant heating rate and frequency were set at, respectively, 4 °C min⁻¹ and 1 Hz. The range of temperature for all the films was from -70 to 140 °C.

3. Results and Discussion

3.1. Latex Synthesis

All the samples synthesized gave a stable latex dispersion with high conversion (>99%). The main characteristics, such as average particle size, molecular weight, and gel content, can be found in **Table 3**. In the latex seeds, two different methods were used for the synthesis, either non-seeded (S series) or seeded (L series) semi-batch emulsion polymerization. As expected, the seeded reactions led to the growth of the seeds, and therefore, the L series of particles has a larger size. The other major difference in the seeds was the composition of the polymer. Samples L_a and S_a consisted of only butyl acrylate and therefore had significant gel content due to intermolecular chain transfer reactions followed by termination by combination as has been reported previously.^[33–35] In samples L_b and S_b, an additional chain transfer agent was added which led to a reduction in the gel content. For reactions with small amounts of a crosslinking agent to the system (L_c and S_c), slightly higher gel contents were observed when compared to L_a and S_a. Finally, a set of small latex seeds containing MMA/BA 30/70 wt/wt (S_d) and MMA/BA 50/50 wt/wt (S_e) in their formulation was synthesized. The gel content of these samples was substantially reduced which may be

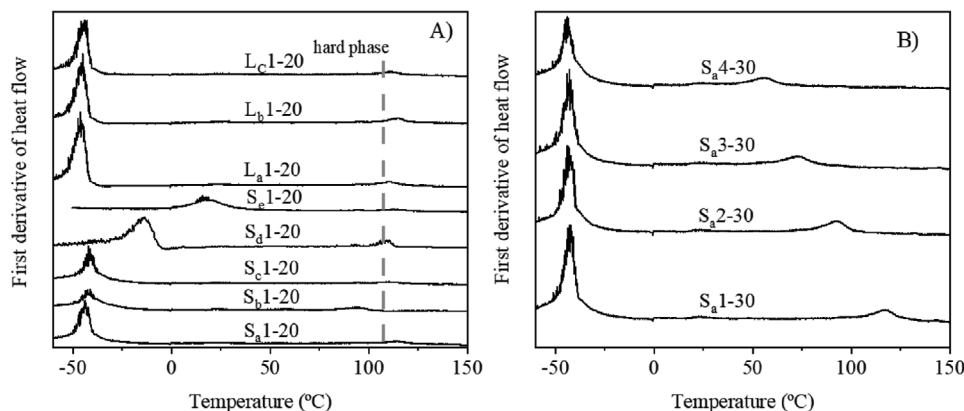


Figure 1. DSC thermograms from the second cycle of two-stage latexes showing A) the effect of changing the composition of the initial poly(butyl acrylate)-rich seed polymer for both small and large latexes and B) the effect of changing the composition of the high T_g second stage polymer.

attributed to a reduction in the extent of intermolecular transfer and increased probability that termination occurs by disproportionation when the fraction of MMA increases.^[36] Since the butyl acrylate-rich seeds make up the majority fraction of the final latexes, these trends are also observed in the final two-stage latexes with a slight reduction in gel content values.

The T_g of the seeds and two-stage latexes was determined via DSC and the results can be found in Table 3 and **Figure 1**. As can be seen in Figure 1, the initial poly(butyl acrylate) seeds have T_g s of approximately -45 °C. No significant differences in the thermal properties were observed comparing the S_a , S_b , and S_c latexes, which are all essentially homopolymers of poly(butyl acrylate). However, for the seeds containing MMA (S_d and S_e), the low T_g peaks are shifted to higher temperatures as expected. For the two-stage latexes, the presence of the hard phase could be detected at high temperatures, although due to the relatively low amounts, the signal was weak compared to that of the BA-rich soft phase. For the case of latexes with a second-stage polymer of composition 1, the hard polymeric phase was composed of MMA/S 85/15, giving T_g values of ≈ 115 °C (see Figure 1A). In samples with second-stage polymer composition 1–4, the composition of the hard phase was changed by varying the content of ethyl acrylate (EA). As expected, the T_g decreased with the increase in the fraction of EA and the sample S_a 4-30 with the highest EA content has a T_g of 52 °C (see Figure 1B).

The morphology of the two-stage latexes containing different relative fractions of the seed and the second-stage polymer was investigated via TEM (see **Figure 2**). It can be noted that in all cases, there was no significant amount of secondary nucleation observed. This is in agreement with the measured particle sizes shown in Table 3, which are in line with the theoretical values assuming no secondary nucleation. The two-stage latexes show distinct morphologies depending on the content of the hard polymer and the particle size of the seed. On the one hand, the two-stage latexes obtained using the large seed had apparently different morphologies depending on the fraction of the hard phase. While a core/shell-like structure was apparent for L_a 1-35 when the amount of second-stage polymer was reduced (sample L_a 1-20), a more “patchy” non-spherical morphology was observed, which implies incomplete shell formation at the particle surface, as has previously been observed.^[30,31]

On the other hand, in the case of the small two-stage latexes, spherical particles were seen and no contrast was observed between the two phases in the TEM, even for the higher content of the hard phase in S_a 1-35 (see Figure 2A,B). Note that the morphology of a small two-stage latex using a non-crosslinked PBA (S_b 1-20) and a crosslinked PBA (S_c 1-20) was also investigated and similar results were observed (see Figure S1, Supporting Information). One reason for the lack of contrast in these samples may be some partial phase mixing at the interface of the two polymers. As previously commented by Dos Santos et al.,^[28] at the interface between two immiscible polymers there is an interphase region in which partial mixing occurs. The interphase profile, $\varphi_i(x)$, as function of distance, x , from the interface, x_0 , can be approximated by

$$\varphi_i(x) = \frac{1}{2} \left(1 + \tanh \frac{x - x_0}{\lambda} \right) \quad (1)$$

where λ is the interphase width given by

$$\lambda = \frac{2a}{\sqrt{6\chi}} Q \quad (2)$$

where χ is the Flory interaction parameter, estimated to be 0.047 for poly(methyl methacrylate) and poly(butyl acrylate) at room temperature,^[37] and a is the monomer length, taken to be 0.6 nm. Taking these values into account and adjusting the value of x_0 such that the correct relative volume fraction of the two phases is reached, the approximate composition profiles for the L_a 1-20 and S_a 1-20 are shown in **Figure 3**.

It can be seen from Figure 3 that for the small particles, the phase mixing model predicts that all the second-stage polymer is contained in the interphase region and therefore the second-stage polymer would be expected to exist in a mixed phase where the T_g is substantially reduced. In contrast, in the case of the larger particles, the interphase region contains only a small fraction of the second-stage polymer. These differences result because the interphase region has a fixed width that accounts for a larger relative volume of polymer in the small particles. These effects of phase mixing cannot be observed in the second cycle DSC thermograms shown in Figure 1, likely due to substantial

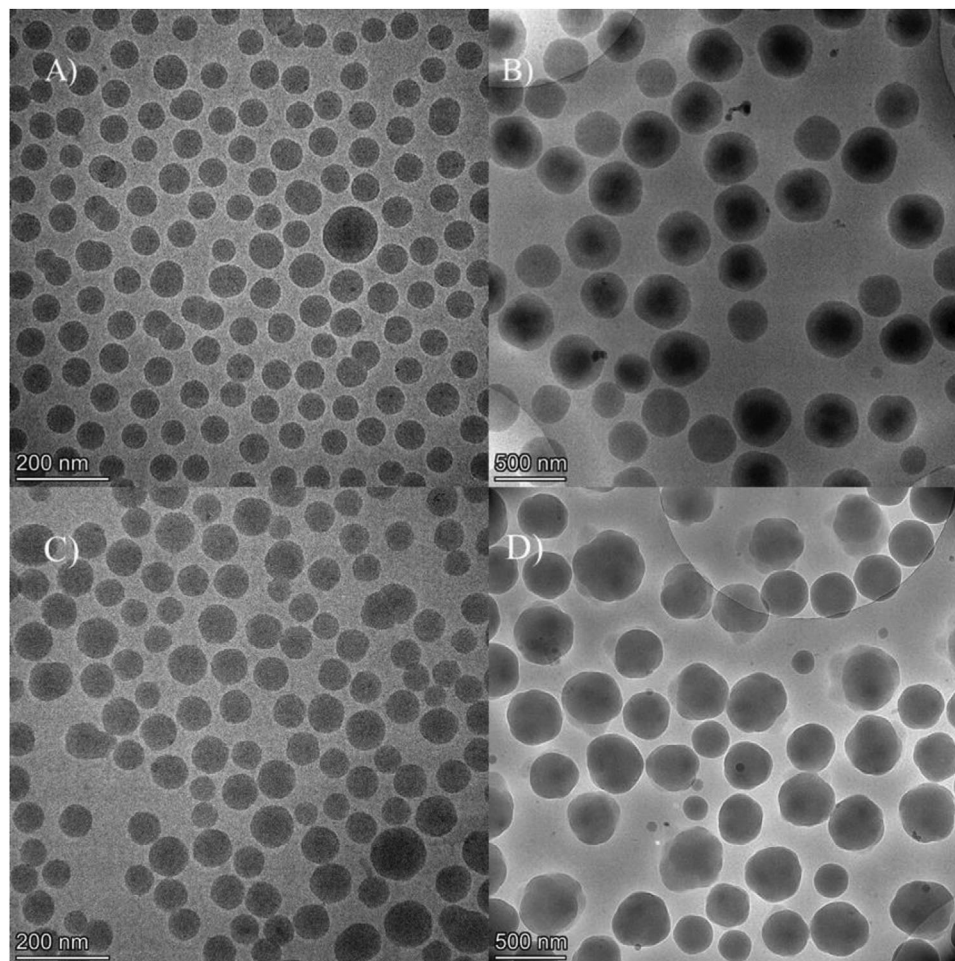


Figure 2. TEM image of two-stage latex particles S_a 1-35 (A), L_a 1-35 (B), S_a 1-20 (C), and L_a 1-20 (D).

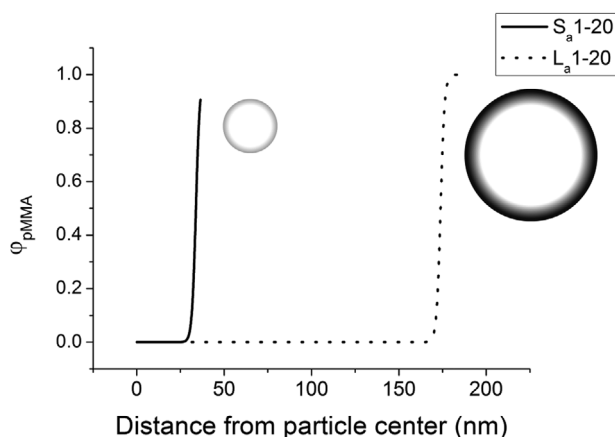


Figure 3. Estimated interphase profile for S_a 1-20 and L_a 1-20 which differ only in the particle size of the initial seed. The spheres show approximate morphologies of the particles with the black phase representing the second-stage polymer assuming a true core/shell structure.

thermal annealing that can occur in the film.^[38] However, phase mixing is clearly visible in the first cycle measurements shown in Figure 4, in which the T_g of the second-stage polymer is significantly reduced. As suggested by the calculated interphase profiles shown in Figure 3, the effects of phase mixing appear to be more important in the case of the smaller two-stage latexes where the interphase region occupies a relatively larger volume.

3.2. Film Formation

3.2.1. Effect of Particle Size of the Seed

Given the apparent difference in particle morphologies and phase mixing as a function of particle size, the film formation of two-stage systems with different particle sizes was then explored. Figure 5 shows the MFFT as a function of the second-stage polymer content for large and small two-stage latexes. As can be seen, dramatic differences in the trends of MFFT were observed for these two systems. Both small and large two-stage latexes had a low MFFT when the fraction of the second-stage polymer was 20%. In the case of small two-stage latexes, there was a sharp increase in the MFFT above this value such that above 20 wt%

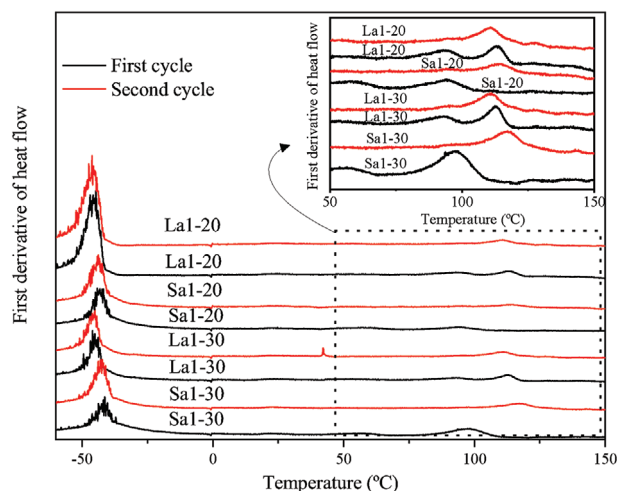


Figure 4. Comparison of first and second-cycle DSC thermograms for latexes S_a 1-20, S_a 1-30, L_a 1-20, and L_a 1-30 showing the shift in the T_g of the higher T_g phase in the second cycle for latexes with lower particle size.

second-stage polymer, film formation at room temperature was not possible. On the other hand, large latexes showed low MFFT values, and the MFFT only increased when the second-stage polymer content reached 35 wt%.

These results can be explained by considering the differences in their particle morphology. For latex L_a 1-20, the TEM images shown in Figure 2D suggest a lobed structure where the second-stage polymer exists in isolated patches as has previously been reported for similar systems.^[30,31] This means that this system does not have a shell fully covering the surface of the seed and therefore deformation of the high T_g phase is not required for film formation and interdiffusion of the soft phase would be possible. As the fraction of the hard phase was increased to 35% in L_a 1-35, a more uniform shell formed on the surface of the particles (see Figure 2B), which would block the deformation and interdiffu-

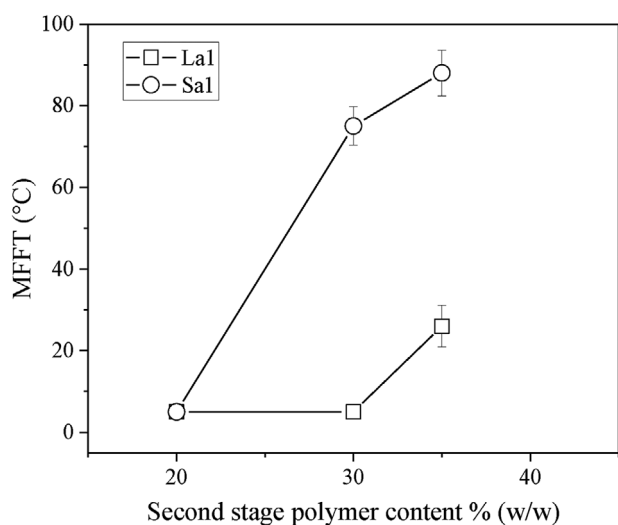


Figure 5. Minimum film formation temperature as a function of the amount of second-stage polymer. The large samples correspond to L_a 1-20, L_a 1-30, and L_a 1-35 and the small samples to S_a 1-20, S_a 1-30, and S_a 1-35.

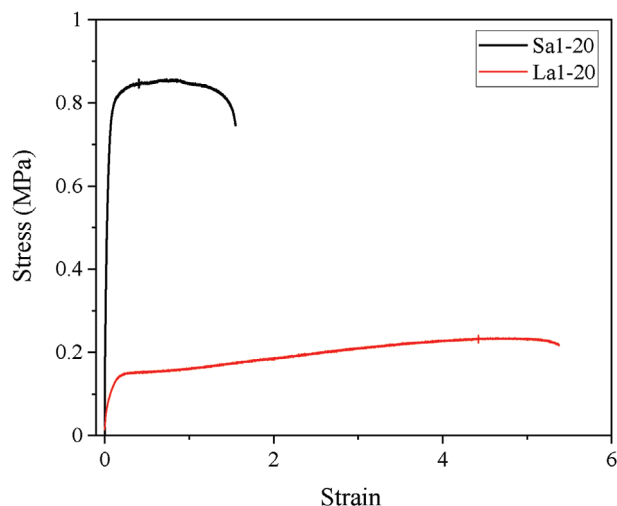


Figure 6. Stress–strain curves from the tensile test of films cast from small (S_a 1-20) and large (L_a 1-20) two-stage latexes.

sion of the soft phase and therefore increase the MFFT. In the case of the small latexes S_a 1-20 and S_a 1-35, the spherical structure observed in the TEM suggests a morphology that is closer to a true core–shell particle which hinders particle deformation and interdiffusion of the soft phase. These latexes are therefore more similar structurally to latexes that are used as redispersable powders, for which film formation is undesirable.^[39–41] However, due to the apparent phase mixing, when the shell is relatively thin, such as in S_a 1-20, the low T_g of the interphase region makes it easier to deform the particle, resulting in a reasonably low MFFT.

Based on the explanation above, the mechanical properties would also be expected to be significantly different depending on the particle size. To prove this, the mechanical properties of the samples able to form a film at temperatures lower than 22 °C (S_a 1-20 and L_a 1-20) were initially investigated in terms of their tensile properties. **Figure 6** shows the stress–strain curves for films prepared using small (S_a 1-20) and large (L_a 1-20) two-stage latexes and the tensile properties of these films are summarized in **Table 4**. Despite having identical overall polymer composition, it can be seen that these systems have significantly different mechanical behavior; the film prepared with the small two-stage latex (S_a 1-20) shows higher Young's modulus and ultimate tensile strength compared to the system prepared using the large two-stage latex (L_a 1-20). However, the opposite was observed for the flexibility of the films and S_a 1-20 exhibits lower elongation at break than L_a 1-20. These trends are in agreement with the arguments outlined above where the more uniform shell assumed for S_a 1-20 would lead to a continuous phase of the high T_g second-stage polymer whereas the patchy structure assumed for L_a 1-20

Table 4. Tensile properties of films cast from small (S_a 1-20) and large (L_a 1-20) two-stage latexes.

Samples	Young's modulus [MPa]	Elongation at break [%]	Ultimate tensile strength [MPa]
S_a 1-20	11.5 (\pm 0.18)	150	0.85
L_a 1-20	2.6 (\pm 0.03)	538	0.23

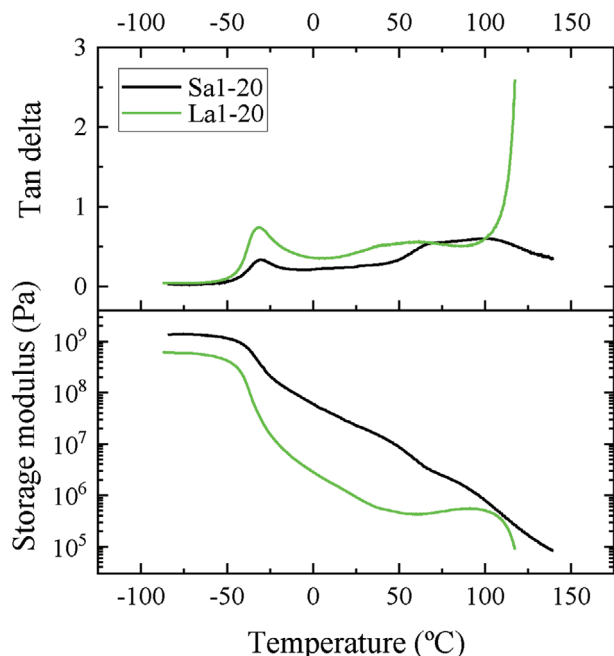


Figure 7. DMTA curves of films cast from small (S_a 1-20) and large (L_a 1-20) two-stage latexes.

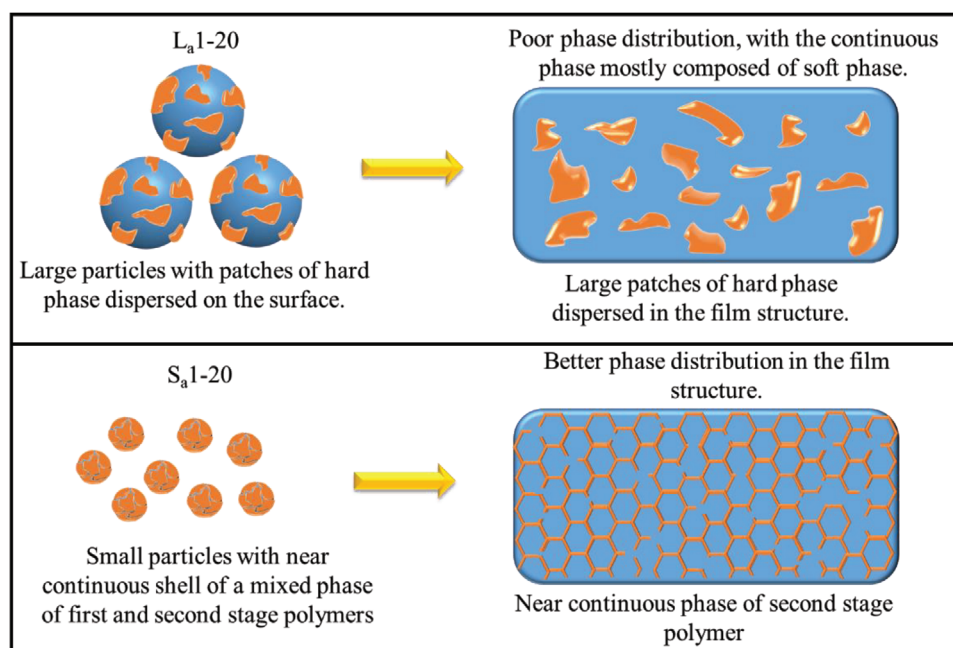
would lead to a more discontinuous network with reduced modulus.

The differences in mechanical properties can also be observed in the thermomechanical properties of S_a 1-20 and L_a 1-20, which were investigated via DMTA as shown in **Figure 7**. The tan (δ) curves show a peak at $-40\text{ }^\circ\text{C}$, which corresponds to the T_g of the soft (PBA) phase. A second T_g corresponding to the second stage

polymer is apparent at high temperatures ($\approx 100\text{ }^\circ\text{C}$), although in the case of S_a 1-20, it is less obvious, which again may be attributed to the higher degree of phase mixing. The main difference in the two samples occurs above the T_g of the soft phase; in the case of L_a 1-20 the storage modulus (G') shows a dramatic decrease at temperatures higher than the T_g of the soft (PBA) phase while this decrease is more gradual for the films of S_a 1-20. These results are again in agreement with the proposed film structure shown in **Scheme 1** in which L_a 1-20 appears as a poly(butyl acrylate) continuous phase with the second-stage polymer dispersed, while S_a 1-20 results in a structure closer to a continuous network of second-stage polymer.

3.2.2. Effect of Second Stage Monomer Composition

The S_a 1-20 system described above is particularly interesting as it appears to demonstrate that as the morphology is closer to a true core/shell-type structure, the mechanical properties are substantially improved. Based on this, the use of varied monomer compositions of the two phases was investigated to try to reach systems with low MFFT but improved mechanical performance. Thus, seed S_a (soft PBA phase) was used to synthesize a series of two-stage latexes where the hard phase fraction was kept at 30% (w/w) but different T_g values of the second-stage polymer were targeted (samples S_a 1-30, S_a 2-30, S_a 3-30, and S_a 4-30). The MFFT plotted as a function of T_g of the second-stage polymer is shown in **Figure 8**. It can be seen that the MFFT decreases with the T_g of the hard phase, with a significant drop in the MFFT for S_a 4-30 (MFFT $< 5\text{ }^\circ\text{C}$). In this case, the T_g is sufficiently reduced such that the particle is capable of deformation at ambient temperature. Note that as expected based on results shown previously, an analogous two-stage latex with identical polymer composition but higher particle size, L_a 4-30,



Scheme 1. Schematic representation of proposed structures of latex S_a 1-20 and L_a 1-20 and their different phase distribution throughout the film structure.

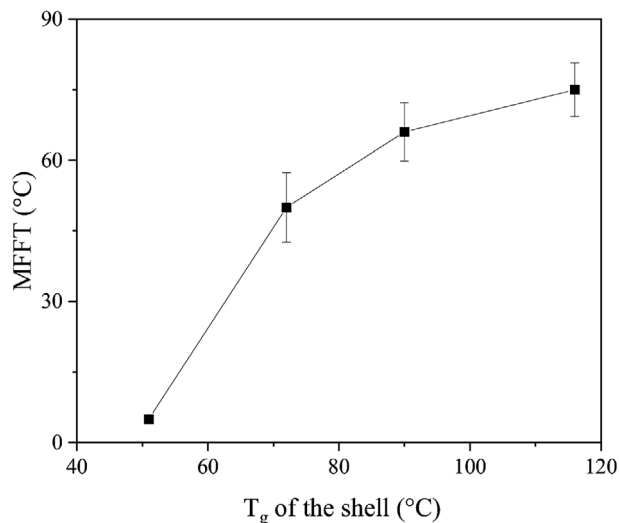


Figure 8. MFFT as a function of hard phase T_g for small two-stage latex particles. The samples correspond to S_a 1-30, S_a 2-30, S_a 3-30, and S_a 4-30.

also had an MFFT that was at the lower limit of measurement (MFFT < 5 °C).

Although by lowering the T_g of the second-stage polymer it was possible to lower the MFFT below room temperature with higher amounts of the second-stage polymer, the improvements in mechanical properties when compared to a system with a lower amount of higher T_g second-stage polymer were negligible. For example, **Figure 9** shows the tensile properties and thermomechanical properties of S_a 1-20 and S_a 4-30. Although latex S_a 4-30 has a higher amount of the second-stage polymer, the lower T_g of the second-stage polymer led to a film with similar mechanical properties to S_a 1-20 at ambient temperature. Moreover, the incorporation of a higher fraction of second-stage polymer in the case of S_a 4-30 led to a decrease in elongation at break. In the DMTA the only major difference was that due to the lower T_g of second-stage polymer in the case of S_a 4-30, there is a substantial drop in the mechanical properties above 50 °C. Thus, these results suggest that the absolute amount of hard phase is less important

than the nature of the phase itself in terms of reinforcing mechanical properties. It may be noted that similar to the results with a lower amount of second-stage polymer (i.e., comparing S_a 1-20 and L_a 1-20 in Figure 7), a significantly higher modulus was observed in the region between the two polymers T_g s when comparing a smaller latex two-stage latex (S_a 4-30) with a larger one (L_a 4-30) (see Figure S2, Supporting Information).

3.2.3. Effect of Seed Monomer Composition

In addition to varying the second-stage polymer composition, the influence of the composition of the polymer seed was also explored. This is particularly important as the use of poly(butyl acrylate) homopolymers leads to low MFFT but also leads to relatively soft films. Seed latexes composed of MMA/BA 30/70 wt/wt (S_d) and MMA/BA 50/50 wt/wt (S_e) were used to synthesize two-stage latexes containing 20 wt% of the second-stage polymer. The MFFT of the two-stage latexes containing a different composition of the soft phase were measured and the results are shown as a function of the glass transition temperature of the seeds in **Figure 10**. It can be seen that the MFFT gradually increased with the T_g of the soft phase and the MFFT was significantly higher than the T_g of the seed latex. This indicates that the second-stage polymer has a strong influence on the film formation behavior, which may be expected due to the core-shell-like structure. Furthermore, as phase mixing would lead to an increase in the T_g of any seed polymer in the interphase region it would be expected that the MFFT would be substantially higher than the T_g of the seed polymer as is observed.

The tensile properties of films cast from S_d 1-20 and S_d 1-20, which have MFFT lower than 22 °C were measured. The results can be seen in **Figure 11** and **Table 5**. The stress-strain curves show that the tensile properties of the film varied significantly with the T_g of the soft phase. The film cast from S_d 1-20 has a higher Young's modulus and ultimate tensile strength than S_a 1-20. However, the elongation at break was very similar in both systems. The thermomechanical properties of both systems can be found in Figure S3, Supporting Information. It can be seen that S_d 1-20 shows a significantly higher modulus than S_a 1-20 up until

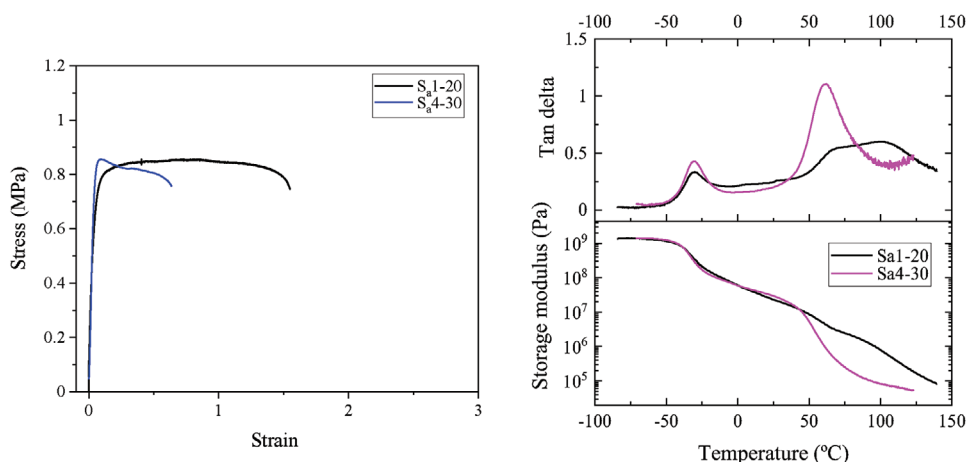


Figure 9. Effect of including a higher amount of lower T_g second stage polymer on the mechanical properties. (Left) Stress-strain curves from the tensile test of films cast from latexes S_a 1-20 and S_a 4-30. (Right) DMTA curves of films cast from latexes S_a 4-30 and S_a 1-20.

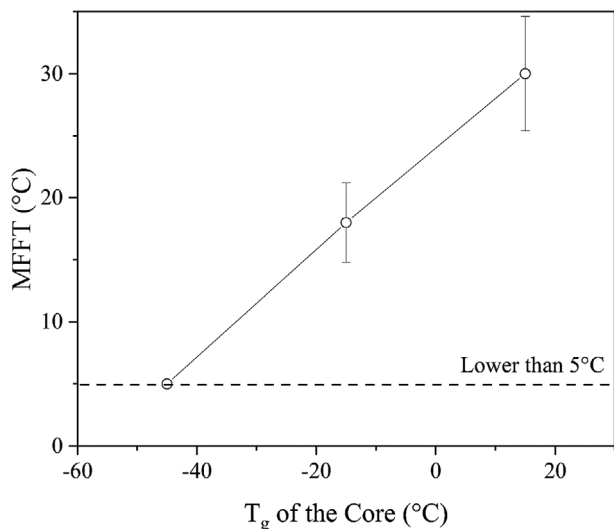


Figure 10. MFFT as a function of hard phase T_g . The samples correspond to latexes S_a 1-20, S_d 1-20, and S_c 1-20.

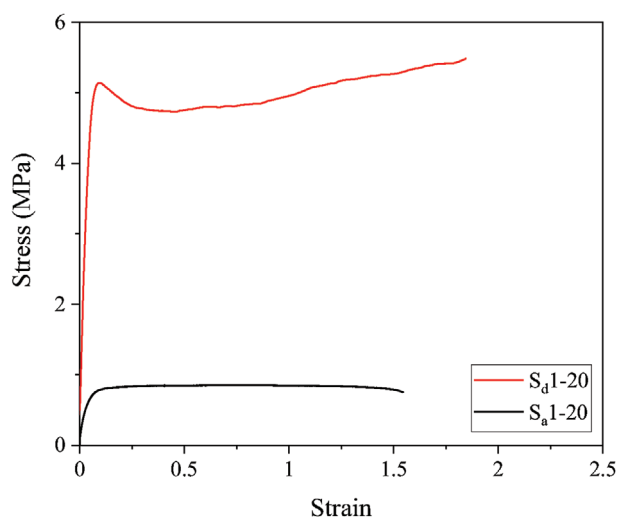


Figure 11. DMTA Curves of S_a 1-20 and S_d 1-20.

the T_g of the second stage polymer. These results show that the mechanical properties of the film can be considerably improved by increasing the T_g of the core, whilst still ensuring a relatively low MFFT. It may also be noted that sample S_d 1-20 has Young's modulus and tensile strength more than an order of magnitude higher than that of films cast from latexes of similar composition but with the inverse hard core/soft shell morphology.^[22]

Table 5. Tensile properties of films cast from two-stage latexes with different compositions of the soft phase.

Samples	Young's modulus [MPa]	Elongation at break [%]	Ultimate tensile strength [MPa]
S_a 1-20	11.5 (\pm 0.18)	150	0.85
S_d 1-20	80.6 (\pm 1.32)	180	5.47

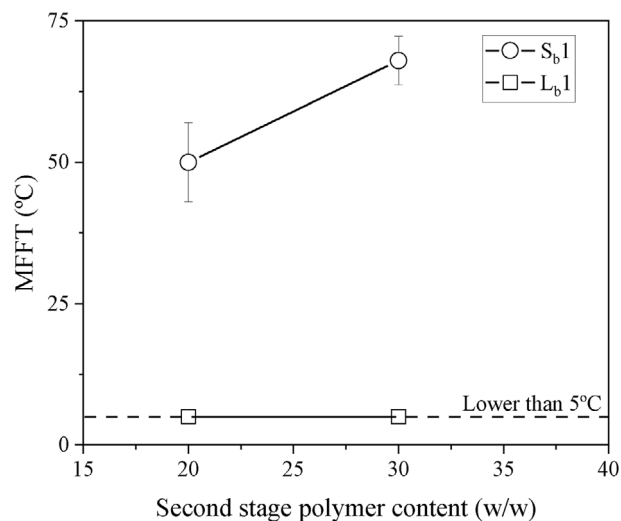
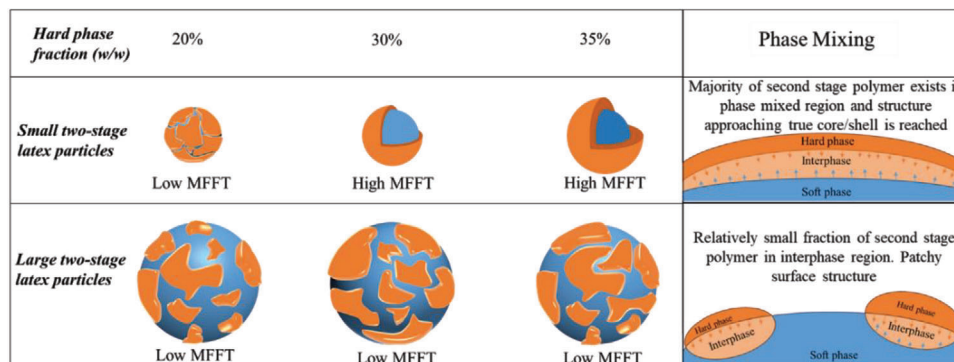


Figure 12. Minimum film formation temperature as a function of the amount of hard phase in two-stage latexes in which the core is synthesized in the presence of a chain transfer agent.

As the composition of the core polymer plays a significant role, both in film formation and in mechanical properties, the effect of crosslinking the initial seed latex was also explored. Crosslinking of the seed would be expected to lead to only limited interpenetration of the low T_g seed polymer but would also result in a higher modulus and more elastomeric character of the film. In order to explore this effect, a series of small and large two-stage latexes were synthesized in which the core was either non-crosslinked (seed S_b by addition of chain transfer agent) or crosslinked (seed S_c by addition of difunctional monomer).

For samples L_c 1-20 and S_c 1-20, where the core was crosslinked, no difference in the MFFT was observed and in both cases the MFFT was at the lower limit of the measurement. In terms of mechanical properties, a slight increase in the modulus was observed in both samples when compared with L_a 1-20 and S_a 1-20 (see Figure S4, Supporting Information). In the case of L_c 1-20, there was a significant reduction in the elongation at break which suggests only a limited degree of interpenetration of the soft seed polymer due to crosslinking. In the case of S_c 1-20, the elongation at break was virtually unaffected which, as commented above, may be related to the mechanical properties being largely dictated by the second-stage polymer.

When a chain transfer agent was added in order to eliminate the formation of gel, surprising results were obtained. It was initially thought that by reducing the extent of network formation in the seed polymer, film formation would be easier, resulting in lower MFFTs. However, as shown in **Figure 12**, whilst the large samples (L_b 1-20 and L_b 1-30) formed a film relatively easily in agreement with the other examples in this work, the smaller two-stage latexes (S_b 1-20 and S_b 1-30) resulted in MFFT > 50 °C, even when the second stage polymer content was low. For these latexes, a seemingly continuous film was formed at temperatures lower than the MFFT, but very small cracks were observed throughout the structure. Given that the low T_g linear poly(butyl acrylate) that forms 80 wt% of the sample should readily form a film, the only clear explanation for this result is that the seed is



Scheme 2. Schematic representation of the variations in the particle morphology of soft-core/hard-shell latexes and the consequences to the film formation properties.

fully encapsulated by the second stage polymer. Crack formation during film formation may therefore be related to the inability of the non-cross-linked, low T_g core to withstand the build-up of stress during film formation. Further evidence for this argument is given by the TEM images of the film cross-section in Figure S5, Supporting Information, which show that the poly(butyl acrylate) (light phase) is apparently dispersed in a network of the second stage polymer.

4. Conclusion

In conclusion, in this work, the film formation behavior of two-stage latex particles synthesized with a high T_g second-stage polymer has been studied. Aiming to obtain film-forming two-stage latexes with low MFFTs, the influence of the seed polymer and the amount and composition of the second-stage polymer were explored. The most significant effect was related to the initial particle size of the seed, which led to apparent differences in the particle morphology as shown in **Scheme 2**. When small seed particles were used, a structure approaching that of a true core/shell system was observed, leading to a more continuous phase of high T_g polymer in the final film and, therefore, superior mechanical properties. However, as a result of this structure, the smaller two-stage latexes also resulted in a significant increase in the MFFT, even when the second-stage polymer content was low. At higher second-stage polymer content, the MFFT could be reduced to values lower than 22 °C by reducing the T_g of the hard phase (shell) but without any significant improvement in the mechanical properties of the film. It was also shown that the mechanical properties of these two-stage latexes could be improved by increasing the T_g of the polymer in the initial seed latex, although the MFFT also increases in this case. In summary, the synthesis of two-stage latexes with small particle sizes offers a route to a film structure that leads to significantly improved mechanical properties whilst maintaining sufficiently low MFFT, even when the amount of high T_g polymer in the system is relatively limited.

Supporting Information

Supporting Information is available from the Wiley Online Library or from the author.

Acknowledgements

The authors would like to acknowledge Sgiker Services of University of the Basque Country and the financial support provided by the Industrial Liaison Program in Polymerization in Dispersed Media (Akzo Nobel, Allnex, Arkema, BASF, Convestro, Elix polymers, Inovyn, Stahl, Synthomer, Vinavil, Wacker, IQLIT, Organik Kimya, Sherwin Williams and TESA).

Conflict of Interest

The authors declare no conflict of interest.

Data Availability Statement

The data that support the findings of this study are available from the corresponding author upon reasonable request.

Keywords

coatings, emulsion polymerization, film formation, latex

Received: August 23, 2023
Revised: September 25, 2023
Published online: November 14, 2023

- [1] B. Richey, M. Burch, in *Polymer Dispersions and Their Industrial Applications*, Wiley-VCH, Weinheim **2002**, pp.123–161.
- [2] S. Jiang, A. Van Dyk, A. Maurice, J. Bohling, D. Fasano, S. Brownell, *Chem. Soc. Rev.* **2017**, *46*, 3792.
- [3] M. Aguirre, N. Ballard, E. Gonzalez, S. Hamzehlou, H. Sardon, M. Calderon, M. Paulis, R. Tomovska, D. Dupin, R. H. Bean, T. E. Long, J. R. Leiza, J. M. Asua, *Macromolecules* **2023**, *56*, 2579.
- [4] J. L. Keddie, A. F. Routh, *Fundamentals of Latex Film Formation*, Springer Science and Business Media, Springer, New York **2010**.
- [5] A. F. Routh, W. B. Russel, *Langmuir* **1999**, *15*, 7762.
- [6] A. Perez, E. Kynaston, C. Lindsay, N. Ballard, *Prog. Org. Coat.* **2023**, *174*, 107246.
- [7] N. Negrete-Herrera, J.-L. Putaux, L. David, F. D. Haas, E. Bourgeat-Lami, *Macromol. Rapid Commun.* **2007**, *28*, 1567.
- [8] K. González-Matheus, G. P. Leal, J. M. Asua, *Polymer* **2015**, *69*, 73.
- [9] D. K. Makepeace, P. Locatelli, C. Lindsay, J. M. Adams, J. L. Keddie, *J. Colloid Interface Sci.* **2018**, *523*, 45.

- [10] L. A. Fielding, J. Tonnar, S. P. Armes, *Langmuir* **2011**, *27*, 11129.
- [11] J. W. Taylor, M. A. Winnik, *JCT Res.* **2004**, *1*, 163.
- [12] M. A. Winnik, *J. Coat. Technol.* **2002**, *74*, 49.
- [13] N. Kessel, D. R. Illsley, J. L. Keddie, *J. Coat. Technol. Res.* **2008**, *5*, 285.
- [14] H. H. Pham, M. A. Winnik, *Macromolecules* **2006**, *39*, 1425.
- [15] M. Argaiz, F. Ruipérez, M. Aguirre, R. Tomovska, *Polymers* **2021**, *13*, 3098.
- [16] Y. Chen, S. T. Jones, I. Hancox, R. Beanland, E. J. Tunnah, S. A. F. Bon, *ACS Macro Lett.* **2012**, *1*, 603.
- [17] H. Wahdat, M. Gerst, S. Möbius, J. Adams, *J. Appl. Polym. Sci.* **2020**, *137*, 48972.
- [18] O. Pinprayoon, R. Groves, P. A. Lovell, S. Tungchaiwattana, B. R. Saunders, *Soft Matter* **2011**, *7*, 247.
- [19] N. Jiménez, N. Ballard, J. M. Asua, *Macromolecules* **2019**, *52*, 9724.
- [20] E. Limousin, N. Ballard, J. M. Asua, *Prog. Org. Coat.* **2019**, *129*, 69.
- [21] A. Pérez, E. Kynaston, C. Lindsay, N. Ballard, *Prog. Org. Coat.* **2022**, *168*, 106882.
- [22] E. L. Brito, N. Ballard, *J. Polym. Sci., Part A: Polym. Chem.* **2023**, *5*, 410.
- [23] B. Schuler, R. Baumstark, S. Kirsch, A. Pfau, M. Sandor, A. Zosel, *Prog. Org. Coat.* **2000**, *40*, 139.
- [24] S. Mehravar, N. Ballard, R. Tomovska, J. M. Asua, *Ind. Eng. Chem. Res.* **2019**, *58*, 20902.
- [25] M. J. Devon, J. L. Gardon, G. Roberts, A. Rudin, *J. Appl. Polym. Sci.* **1990**, *39*, 2119.
- [26] A. Perez, E. Kynaston, C. Lindsay, N. Ballard, *Polym. Chem.* **2022**, *13*, 5636.
- [27] E. Limousin, N. Ballard, J. M. Asua, *J. Appl. Polym. Sci.* **2019**, *136*, 47608.
- [28] F. Domingues Dos Santos, P. Fabre, X. Drujon, G. Meunier, L. Leibler, *J. Polym. Sci., Part B: Polym. Phys.* **2000**, *38*, 2989.
- [29] F. Domingues Dos Santos, L. Leibler, *J. Polym. Sci., Part B: Polym. Phys.* **2003**, *41*, 224.
- [30] F. Sommer, T. M. Duc, R. Pirri, G. Meunier, C. Quet, *Langmuir* **1995**, *11*, 440.
- [31] H. Abdeldaim, B. Reck, K. J. Roschmann, J. M. Asua, *Macromolecules* **2023**, *56*, 3304.
- [32] H. Abdeldaim, J. M. Asua, *Chem. Eng. J.* **2023**, *473*, 145270.
- [33] C. Plessis, G. Arzamendi, J. R. Leiza, H. A. S. Schoonbrood, D. Charmot, J. M. Asua, *Macromolecules* **2000**, *33*, 5041.
- [34] C. Plessis, G. Arzamendi, J. R. Leiza, H. A. S. Schoonbrood, D. Charmot, J. M. Asua, *Ind. Eng. Chem. Res.* **2001**, *40*, 3883.
- [35] N. Ballard, S. Hamzehlou, J. M. Asua, *Macromolecules* **2016**, *49*, 5418.
- [36] I. González, J. M. Asua, J. R. Leiza, *Polymer* **2007**, *48*, 2542.
- [37] A.-V. Ruzette, S. Tencé-Girault, L. Leibler, F. Chauvin, D. Bertin, O. Guerret, P. Gérard, *Macromolecules* **2006**, *39*, 5804.
- [38] A. K. Tripathi, J. G. Tsavalas, D. C. Sundberg, *Thermochim. Acta* **2013**, *568*, 20.
- [39] A. Zaroni, C. Casiraghi, R. Po, P. Biagini, M. Sponchioni, D. Moscatelli, *Macromol. Mater. Eng.* **2023**, *308*, 2200443.
- [40] S. Caimi, E. Timmerer, M. Banfi, G. Storti, M. Morbidelli, *Polymers* **2018**, *10*, 1122.
- [41] F. Wang, Y. Luo, B. o.-G. Li, S. Zhu, *Macromolecules* **2015**, *48*, 1313.